

A COMPREHENSIVE STUDY ON THE EFFICIENCY OF THREE DIFFERENT TYPES OF THE VARIABLE METRIC METHOD IN DETERMINING THE UNKNOWN ROCKET INNER HEAT FLUX

H. Khoshkam^{1*}, M. Beyrami², K. Javaherdeh³

^{1,3}Iran Faculty of Engineering, Department of Mechanical Engineering, University of Guilin
²Department of Mechanical Engineering, Asadabad Branch, Islamic Azad University, Asadabad

ABSTRACT

In this paper, the unknown heat flux is estimated with Davidon-Fletcher-Powell (DFP), Broydon-Fletcher-Goldfarb-Shanno (BFGS) and Symmetric Rank-one (SRI) version of variable metric method (VMM). The numerical techniques used in this study solved the inverse problems with various boundary and environmental conditions so efficiently. The results shows the sensitivity of measurement errors and different parameter including changes of slope and angle which can be functions of an unknown parameter. Further, the speed of convergence is assessed and the convergence behavior is found. The accuracy of results show that this study is a powerful reference for comparing results obtained based on the three proposed techniques. The solution procedure introduced a general fast method which can be used for the inverse heat conduction problem in rocket nozzle and same heat conduction, radiation and convection problems.

KEYWORDS: BFGS; SRI; DFP; Rocket nozzle; Heat conduction; VMM method; Inverse problem

1.0 INTRODUCTION

The nozzle plays an important role in the rocket motor, as the equipment of converting energy and producing thrust force for rocket, it converts the thermal energy of gases into the kinetic energy. During the motor operation process, the nozzle must endure the impact of jet flow with high temperature and pressure. The high temperature from the inner contour of the nozzle conducted into its shell leads to the increase and decrease of the erosion of nozzle throat insert and the material strength of the nozzle shell, respectively. Additionally, it enlarges the throat radius which makes thrust descend, and also reduces the nozzle thrust efficiency. Under these situations, the nozzle design obviously affects the motor performance. Evaluation of rocket nozzle safety and its reliability can be assessed through numerical analysis of heat transfer and wall temperature. In order to meet the requirements in resisting the nozzle shell temperature and the jet flow, the throat-insert materials need to be inserted in the nozzle inner counter to form protection. There are three major material requirements, which are the throat-insert, thermal liner and insulator materials (Tsung-Chien Chen & Chiun-Chien Liu, 2008).

* Corresponding author e-mail: hamed.khoshkam@gmail.com

The nozzle throat which consists of an expensive super alloy, will directly affect the nozzle efficiency and is very effective for reduction of the running costs of a power generation plant. Accordingly, it is very important for the life assessment of the nozzle to predict the operating conditions and to establish a basis for the criteria of repair. Therefore, the heat conduction problem design in the nozzle and the method to choose moderate throat-insert materials are of the essential importance indeed (H.N. Wang & J.H. Wang, 2006). As a result, the estimation of heat flux in the rocket nozzle throat in high temperature environment is a crucial building block for assessing the safety and reliability of the nozzle.

The inverse heat conduction problem is concerned with different parameters. Among these parameters, one can refer to the thermal conductivity, the volumetric heat capacity, the initial condition, the boundary conditions, and the heat sources from knowledge of the temperature or heat flux measurements taken at the interior point of the solid or on its back surface (G. Stolz, Jr., 1960). Solution methods of the inverse heat transfer problems (IHTP) for heat flux estimation can generally be classified into two categories: sequential methods and whole domain methods. Both of these two categories involve minimization of a sum of squares of errors function defined on the basis of the difference between measured and calculated temperatures. In the sequential function (SFS) method (J. V. Beck, B. Blackwell and C.R. St. Clair, 1985), which is the most noted algorithm of the first group, unknown heat fluxes are estimated in a consecutive manner. That is, the algorithm is based on marching in time and determining the unknown heat flux in current time step using future data by setting the derivative of the error function with respect to unknown heat fluxes equal to zero. In the whole domain methods, in which all of the known heat fluxes are estimated simultaneously, the minimization of the sum of squares of error function is achieved by the iterative minimization (optimization) techniques (J.G. Bauzin & N. Laraqi, 2004). One of these techniques is called the variable metric method (VMM). The VMM has superior characteristics as compared to the conjugate gradient method. The VMM is a powerful technique in the context of nonlinear optimization problems. This method has been utilized in the solution of inverse problems (M. Prud'homme & S. Jasmin, 2003). In this paper, a comprehensive discussion on DFP, BFGS and SR1 is presented for estimating the unknown boundary heat flux based on the boundary temperature measurements history that is measured at outside the body. Furthermore, three examples are employed to demonstrate and discuss results of the three version of VMM in detail in the following sections (H.Khoshkam & M.Alizadeh, 2011).

2.0 THE DIRECT PROBLEM

The specimen is a nozzle throat (see Figure 1) this slab originally has a uniformly distributed temperature. A heat flux $q(t)$ is applied to $x = l$ at a specific time ($t > 0$), convective heat flux at $x = 0$ with constant Heat transfer coefficients at the constant temperature. The following hypotheses have been taken into account:

- 1- Thermo-physical properties are assumed to be constant.
- 2- Heat transfer is one-dimensional.
- 3- Heat transfer coefficients are constant.
- 4- Radiation is not important.

Under these conditions, the heat transfer process in the specimen can be described by the following system of equations:

$$k \frac{\partial^2 T}{\partial x^2} = \rho c \frac{\partial T}{\partial t} \quad 0 \leq x \leq 1 \quad \text{and} \quad t \geq 0 \quad (1)$$

$$T(x, t) = T_0 \quad 0 \leq x \leq 1 \quad \text{and} \quad t = 0 \quad (2)$$

$$-k \frac{\partial T(x, t)}{\partial x} = h(T - T_\infty) \quad x = 0 \quad \text{and} \quad t > 0 \quad (3)$$

$$k \frac{\partial T(x, t)}{\partial x} = q(x, t) \quad x = 1 \quad \text{and} \quad t > 0 \quad (4)$$

Here k , ρ and c are the thermal conductivity, density, heat and capacity, respectively.

The governing equation is parabolic and the solution for the above heat conduction problem is solved by using finite volume method (S.V. Patankar, 1980).

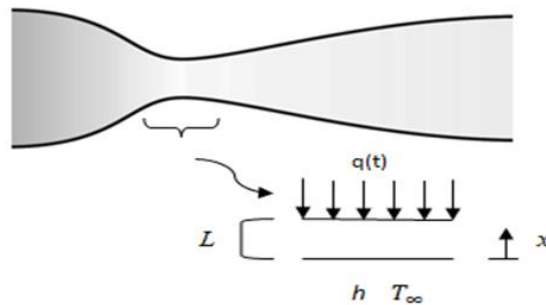


Figure 1. The one-dimensional rocket nuzzle throat geometry

3.0 SIMULATED INEXACT MEASUREMENT

The measured temperature data must contain measurement errors. a normally distributed uncorrelated error with zero mean and constant standard deviation are considered, In order to compare the results for situations involving random measurement errors can be expressed as:

$$Y = Y_{\text{exact}} + \omega \sigma \quad (5)$$

Where Y_{exact} and Y in Equation(5) are the solution of the direct problem with an exact boundary heat flux $q(1, t)$ and the measured temperature, respectively. Furthermore, ω is the random variable with normal distribution, zero mean and unitary standard deviation and for the 99% confidence bound we have (Ch. H. H. & H. H. Wu, 2006) $-2.576 < \omega < 2.576$

3.1 INVERSE PROBLEM

In this inverse problem the heat flux $q(t)$ is unknown; and the unknown heat flux find by the VMM method stated below the boundary heat flux at $x = 1$ is regarded as being unknown, but everything else in Equations (1)–(4) is known. In addition, temperature readings at $x = 0$ are considered available. The temperature reading taken by sensors at $x = 0$ be denoted by $Y(0, t)$, it is noted that the measured temperature $Y(0, t)$ contain measurement errors. With the above mentioned measured temperature data $Y(0, t)$, the method estimate the unknown boundary heat flux $q(1, t)$ in such a way that the following functional is minimized:

$$f = \sum_{k=1}^K \sum_{m=1}^M [Y(x_k, t_m) - T(x_k, t_m, q_m)]^2 \quad (3)$$

In the above definition, K is total number of sensors, Y is the measured temperature at sensor location of x_k , and T is the calculated temperature utilizing the direct heat conduction model (Equation 1) based on a given or assumed vector for \vec{q} .

4.1. Variable Metric Method (VMM)

The variable metric method (VMM), belong to the gradient optimization techniques. It can minimize the object function through an iterative procedure. The variable metric method is very stable and continues to progress towards the minimum even when dealing with highly distorted and eccentric functions. The steepest descent method, the conjugate gradient method, the Newton method and the variable metric method (VMM), all belong to the gradient based class of unconstrained optimization techniques. However, VMM has superior characteristics in relation to the others (F. Kowsary, A. Behbahaninia, A. Pourshaghaghay, 2006). The variable metric method is very stable and continues to progress towards the minimum even when dealing with highly distorted and eccentric functions. Zhang et al. demonstrated mathematically that for a strictly convex quadratic objective function, the generated iterative sequence of VMM converges to the unique solution of the problem globally and super linearly (Z.Z. Zhang, D.H. Cao, J.P. Zeng, 2004). The iterative procedure for the VMM can be summarized as follows:

Step 1: Find the pulse sensitivity coefficients for each components of \vec{q} by solving Equations (6) – (9) in the entire time domain.

Step 2: At the start an initial guess for \vec{q} and with a $M \times M$ positive definite symmetric matrix H_1 (M is total number of unknowns). H_1 is taken as the identity matrix I . Set iteration number as $i=1$.

Step 3: Compute the gradient of the objective function, $\vec{\nabla} f_i$; (defineat below) at the base point \vec{q}_i ; and define search direction as: $\vec{S}_i = -H\vec{\nabla} f_i$

Step 4: Normalize S_i by its magnitude: $\vec{S}_i = \vec{S}_i / \|\vec{S}_i\|$

Step 5: compute the optimal step length λ_i^* in the direction \vec{S}_i and achieve to the next \vec{q}_i using: $\vec{q}_{i+1} = \vec{q}_i + \lambda_i^* \vec{S}_i$

Step 6: Test the new \vec{q}_{i+1} for optimality. If \vec{q}_{i+1} is optimal, terminate the iteration process. Otherwise, go to step (7).

Step 7: Update the ((H)) matrix

Step 8: Set the new iteration number $i=i+1$, and go to step 3

"M" is total number of time steps that cover the entire time domain and the unknown heat flux $q(t)$ is discretized into M time components. All the components are gathered inside a vector \vec{q} as:

$$\vec{q} = [\vec{q}(t_1), \vec{q}(t_2), \dots, \vec{q}(t_M)] \quad (4)$$

For Kth sensors, sensitivity coefficient of measured temperature is obtained with respect to each $q_{\tilde{m}}$:

$$X(x_k, t_m, q_{\tilde{m}}) = \frac{dT(x_k, t_m)}{dq_{\tilde{m}}} \quad \text{for } \tilde{m}=1, 2, \dots, M \quad (5)$$

$$\frac{\partial^2 X}{\partial x^2} = \frac{1}{\alpha} \frac{\partial X}{\partial x} \quad (6)$$

$$\frac{\partial X}{\partial x} = -hX \quad (7)$$

$$k \frac{\partial X}{\partial x} = \begin{cases} 1 & \text{if } t_{m-1} \leq t < t_m \\ 0 & \text{other } t \end{cases} \quad (8)$$

$$X(x_i, t \leq t_{m-1}) = 0 \quad \text{for } \tilde{m}=1, 2, \dots, M \quad (9)$$

The above equation should also be solved separately for every M time in order to compute $X(x_k, t_m, q_{\tilde{m}})$.

The Gradient of objective function which must be minimized used in VMM has the form of:

$$\vec{\nabla} f_{n \times 1} = \left[\frac{\partial f}{\partial q_1}, \frac{\partial f}{\partial q_2}, \dots, \frac{\partial f}{\partial q_n} \right]^T \quad (10)$$

And from the Equation (10) we can write $\vec{\nabla} f_i$ as:

$$\vec{\nabla} f_{n \times 1} = \begin{bmatrix} -2 \sum_{k=1}^k \sum_{m=1}^M ([Y(x_k, t_m) - T(x_k, t_m, q_{\tilde{m}})] X(x_k, t_m, q_1)) \\ -2 \sum_{k=1}^k \sum_{m=1}^M ([Y(x_k, t_m) - T(x_k, t_m, q_{\tilde{m}})] X(x_k, t_m, q_2)) \\ \vdots \\ -2 \sum_{k=1}^k \sum_{m=1}^M ([Y(x_k, t_m) - T(x_k, t_m, q_{\tilde{m}})] X(x_k, t_m, q_M)) \end{bmatrix} \quad (11)$$

In step (5) of VMM, the optimal step size (λ_i^*) in the direction of S_i is a value of λ_i^* that minimizes $f(\vec{q}_i + \lambda_i^* \vec{S}_i)$ with respect to λ_i^* i.e., λ_i^* is the root of the following equation:

$$\frac{df(\vec{q}_i + \lambda_i^* \vec{S}_i)}{d\lambda_i^*} = 0 \quad (12)$$

For the stopping criteria (step 8); In this work $\|f\| \leq \varepsilon$ is used as the stopping criteria, In the case of non-noisy data, ε is an arbitrary small number (in this work $\varepsilon = 0.001$). But in the case of noisy data, ε should be chosen based on the iterative regularization method in order to reduce sensitivity of the solution to the random noise errors. The main idea in the iterative regularization is to stop the iterative procedure close but not exactly at the optimum point. Then, it will tend to regularize the solution and to damp out the destructive effects of random noises in data.

$$\varepsilon = k \times M \times A^2 \quad (13)$$

But in this work we use $\varepsilon = 3$ for noisy data because it has better results. Different version of VMM has a different way to update the H (step7). Symmetric Rank-one (SR1) update by:

$$H_{i+1} = H_i + \left(1 - \frac{Q_i^T H_i Q_i}{Q_i^T (\lambda_i^* S_i)}\right)^{-1} * \frac{1}{Q_i^T (\lambda_i^* S_i)} (\lambda_i^* S_i - H_i Q_i)(\lambda_i^* S_i - H_i Q_i)^T \quad (14)$$

Davidon-Fletcher-Powell (DFP) :

$$H_{i+1} = H_i + \lambda_i^* \frac{S_i S_i^T}{S_i^T Q_i} - \frac{(H_i Q_i)(H_i Q_i)^T}{Q_i^T H_i Q_i} \quad (15)$$

Broydon-Fletcher-Goldfarb-Shanno (BFGS):

$$H_{i+1} = H_i + \lambda_i^* \frac{S_i S_i^T}{S_i^T Q_i} - \frac{(H_i Q_i)(H_i Q_i)^T}{Q_i^T H_i Q_i} + \dots \dots \dots + (Q_i^T H_i Q_i) * \left(\frac{S_i}{S_i^T Q_i} - \frac{H_i Q_i}{(Q_i^T H_i Q_i)}\right) \left(\frac{S_i}{S_i^T Q_i} - \frac{H_i Q_i}{(Q_i^T H_i Q_i)}\right)^T \quad (16)$$

5.0 RESULTS AND DISCUSSIONS

Our simulations define from Eqs. (1) – (4) that estimates the strength of the boundary heat flux. To illustrate the accuracy of the BFGS, SR1 and DFP in predicting boundary heat flux $q(l, t)$ with the present inverse analysis, three different boundary heat flux functions over temporal domain; namely, a third degree polynomial function, triangular function and a step function are adopted to illustrate the numerical modeling. The exact temperature and the heat flux used in the following examples are selected so that these functions can satisfy Eqs. (1) – (4).

$$q(l, t)_{\text{Initial}} = 0$$

The following computational parameters are chosen for the numerical experiments:

$$\begin{aligned} T_0 &= 25 \text{ }^\circ\text{C}, \\ T_\infty &= 25 \text{ }^\circ\text{C}, \\ l &= 0.01 \text{ m}, \\ k &= 138 \text{ W/ (m.k) }, \\ \alpha &= 5.369 \times 10^{-5} \text{ m}^2 / \text{s}, \\ h &= 5000 \text{ W/ (m}^2 \text{ k)} \end{aligned}$$

Here α is the thermal diffusivity of the material. Besides, the space and time increments used in numerical calculations are taken as $\Delta x = 0.00001 \text{ m}$ (i.e. 1000 grid points in space) and $\Delta t = 1 \text{ s}$ (i.e. 30 grid points for $t_f = 30 \text{ s}$). We now present below three numerical test cases in determining $q(l, t)$ by the inverse analysis using the different version of the VMM.

Numerical Test-Case 1: The unknown transient boundary heat flux $q(l, t)$ is assumed applied at $x = l$ in the following form:

$$q(l, t) = -252.5t^3 + 1.547 \times 10^4 t^2 - 3.475 \times 10^5 t + 3.26 \times 10^6 \quad (17)$$

The relative root mean square error (e_{RMS}) for the estimated $q(l, t)$ is defined as:

$$e_{RMS} = \frac{\sqrt{\frac{1}{N} \sum_{I=1}^N [q(l, t) - \bar{q}(l, t)]^2}}{\sqrt{\frac{1}{N} \sum_{I=1}^N [q(l, t)]^2}} \times 100\% \quad (18)$$

Where I and N represent the index of discrete time and total number of measurements, respectively, while $\bar{q}(l, I)$ denote the estimated values of heat flux.

Table 1. Root mean square error and convergence criteria for estimating heat flux to the third degree polynomial.

	Number of Iterations	e_{RMS}	Run time (s)	$ \nabla f $ at final
DPF $\sigma \approx 0^\circ\text{C}$	26	9.70	11.07	3.91×10^{-6}
SR1 $\sigma \approx 0^\circ\text{C}$	22	9.71	10.81	3.68×10^{-6}
BFGS $\sigma \approx 0^\circ\text{C}$	23	9.69	10.56	3.21×10^{-6}
DPF $\sigma = 3^\circ\text{C}$	13	11.75	8.62	3.34×10^{-4}
SR1 $\sigma = 3^\circ\text{C}$	12	11.86	8.21	2.28×10^{-4}
BFGS $\sigma = 3^\circ\text{C}$	12	11.25	8.18	3.12×10^{-4}
DPF $\sigma = 10^\circ\text{C}$	17	39.81	9.35	6.34×10^{-4}
SR1 $\sigma = 10^\circ\text{C}$	14	45.88	8.32	7.59×10^{-4}
BFGS $\sigma = 10^\circ\text{C}$	14	31.02	8.94	4.35×10^{-4}

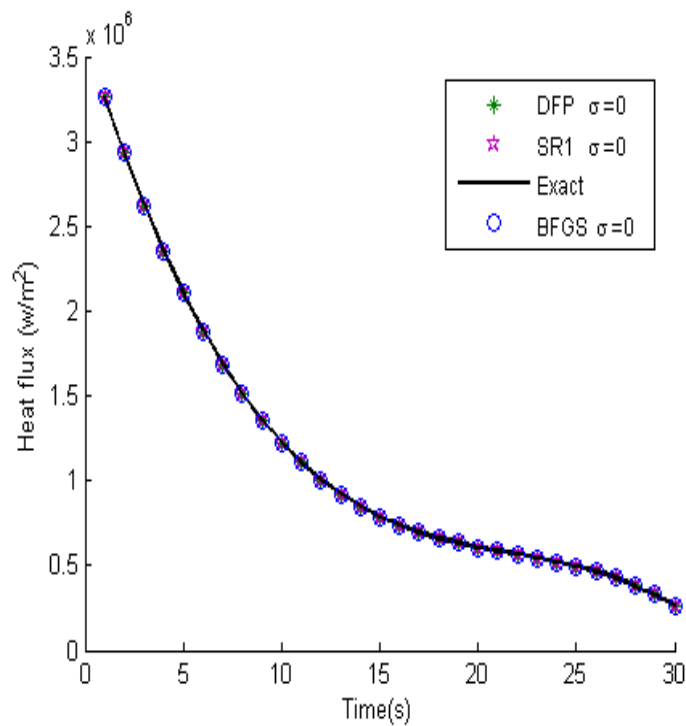


Figure 2. The estimation of the third degree polynomial heat flux with $\sigma = 0$

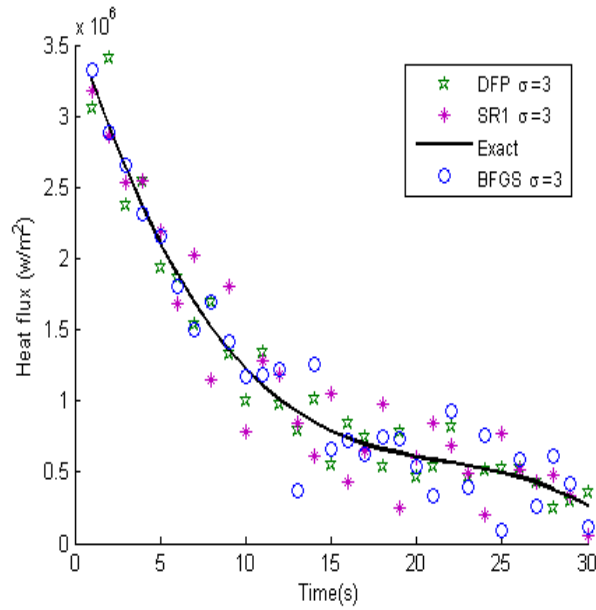


Figure 3. The estimation of the third degree polynomial heat Flux with $\sigma = 3$

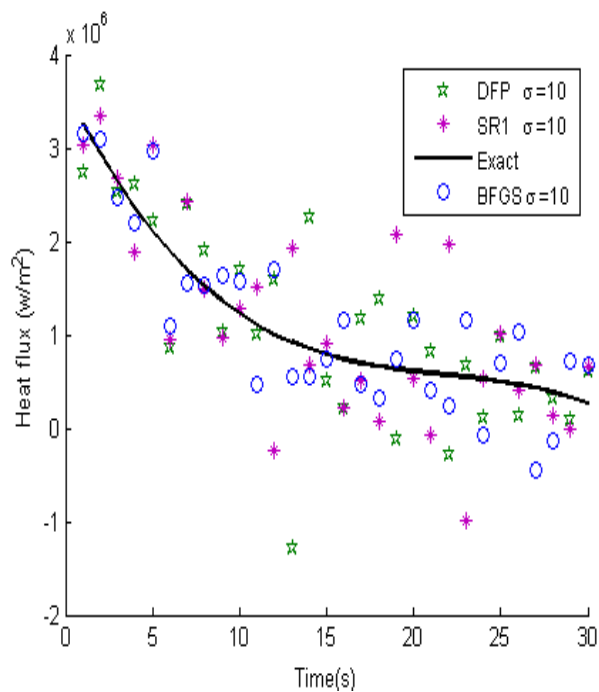


Figure 4. The estimation of the third degree polynomial heat Flux with $\sigma = 10$

Table 2. Root mean square error and convergence criteria for estimating triangular heat flux

	Number of Iterations	e_{RMS}	Run time (s)	$\ \nabla f\ $ At final
DPF $\sigma \approx 0^\circ\text{C}$	24	12.56	10.88	$3.26 \cdot 10^{-6}$
SR1 $\sigma \approx 0^\circ\text{C}$	20	12.55	10.25	$3.62 \cdot 10^{-6}$
BFGS $\sigma \approx 0^\circ\text{C}$	20	12.55	10.25	$4.83 \cdot 10^{-6}$
DPF $\sigma = 3^\circ\text{C}$	9	12.67	7.45	$3.26 \cdot 10^{-4}$
SR1 $\sigma = 3^\circ\text{C}$	10	14.18	8.10	$3.33 \cdot 10^{-4}$
BFGS $\sigma = 3^\circ\text{C}$	10	12.80	7.78	$3.67 \cdot 10^{-4}$
DPF $\sigma = 10^\circ\text{C}$	15	30.17	11.35	$7.19 \cdot 10^{-4}$
Sr1 $\sigma = 10^\circ\text{C}$	14	38.09	11.32	$8.91 \cdot 10^{-4}$
BFGS $\sigma = 10^\circ\text{C}$	14	36.63	9.15	$6.27 \cdot 10^{-4}$

Figure 2 to Figure 4 and Table 2 show that in the third degree polynomial heat flux, if the measurement error for the temperatures, measured by sensor, is $\sigma = 0^\circ\text{C}$, each of the three version of VMM converge very rapidly and exact enough to the real heat flux and have a same root mean square error, but BFGS and SR1 are faster than DFP. In $\sigma = 3$ DFP and BFGS have a good root mean square error, However, SR1 and BFGS converge faster than DFP. In large measurement errors BFGS have faster and more accuracy answers than two other version.

Numerical Test-Case 2: The unknown boundary heat flux $q(l,t)$ is assumed applied at $x=1$ in the following form:

$$q(1, t) = \begin{cases} 0 & 0 < t \leq 1 \\ \frac{10^6 t - 10^6}{5} & 1 < t \leq 16 \\ \frac{-10^6 t + 29 \times 10^6}{5} & 16 < t \leq 30 \end{cases} \quad (17)$$

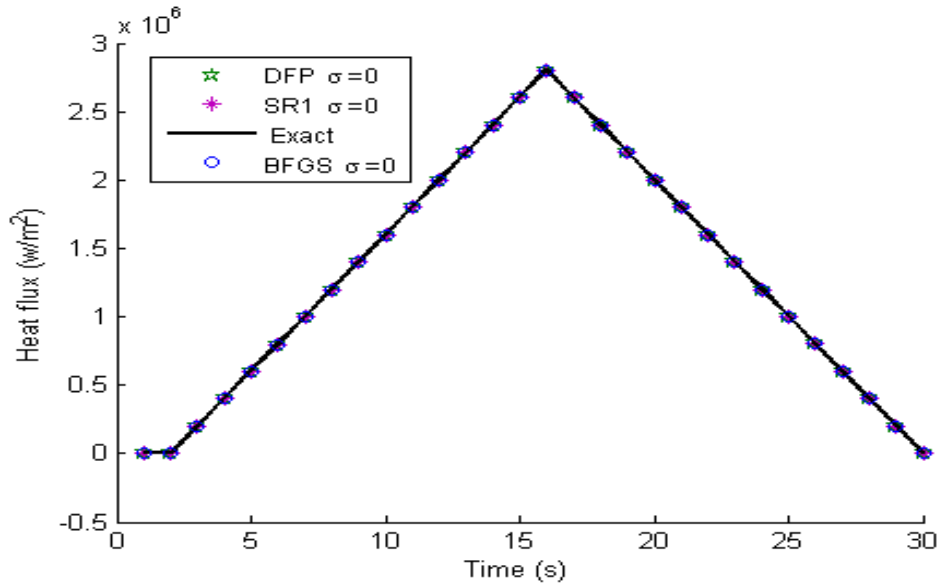


Figure 5. The estimation of the triangular heat flux with $\sigma = 0$

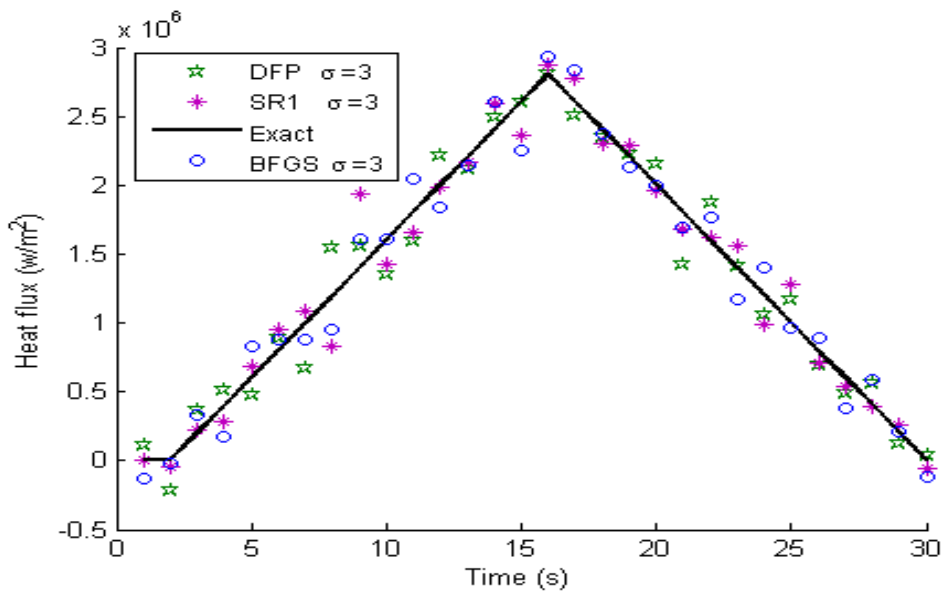


Figure 6. The estimation of the triangular heat flux with $\sigma = 3$

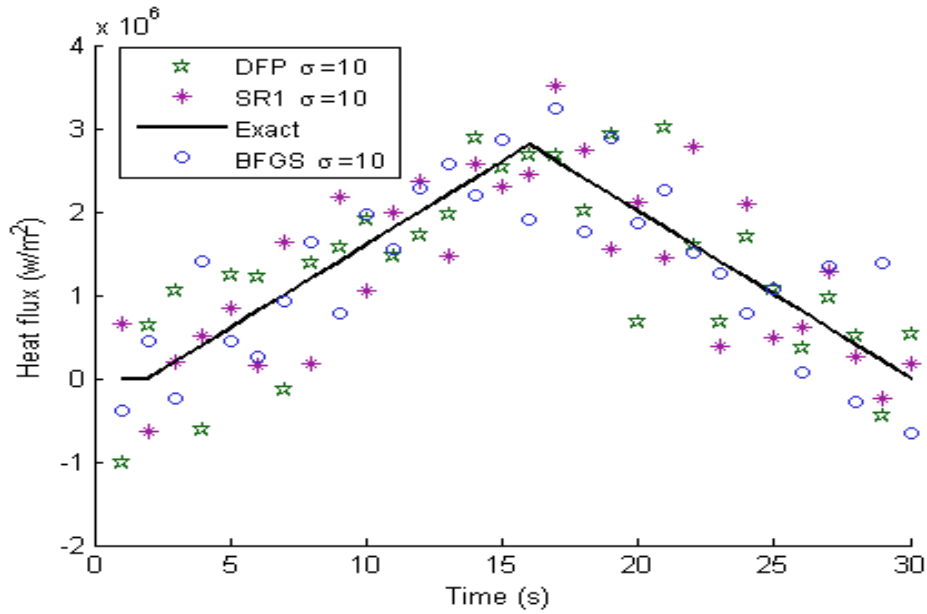


Figure 7. The estimation of the triangular heat flux with $\sigma = 10$

Numerical Test-Case 3: The unknown boundary heat flux $q(l, t)$ is assumed applied at $x = l$ in the following form:

$$q(l, t) = \left\{ \begin{array}{ll} 0 & 0 \leq t \leq 16 \\ 3.6 \times 10^6 & 16 < t \leq 30 \end{array} \right\} \quad (17)$$

Table 3. Root mean square error and convergence criteria for estimating step heat flux

	Number of Iterations	e_{RMS}	Run time (s)	$ \nabla f $ at final
DPF $\sigma \approx 0^\circ\text{C}$	33	0.25	12.07	$2.10 \cdot 10^{-6}$
SR1 $\sigma \approx 0^\circ\text{C}$	28	0.20	10.72	$4.01 \cdot 10^{-6}$
BFGS $\sigma \approx 0^\circ\text{C}$	28	0.18	10.92	$2.01 \cdot 10^{-6}$
DPF $\sigma = 3^\circ\text{C}$	17	7.77	9.16	$3.68 \cdot 10^{-6}$
SR1 $\sigma = 3^\circ\text{C}$	16	8.45	8.67	$2.09 \cdot 10^{-4}$
BFGS $\sigma = 3^\circ\text{C}$	16	6.47	8.42	$3.39 \cdot 10^{-4}$
DPF $\sigma = 10^\circ\text{C}$	17	21.54	8.62	$7.19 \cdot 10^{-4}$
Sr1 $\sigma = 10^\circ\text{C}$	16	25.55	8.72	$3.41 \cdot 10^{-4}$
BFGS $\sigma = 10^\circ\text{C}$	16	29.27	8.91	$4.41 \cdot 10^{-4}$

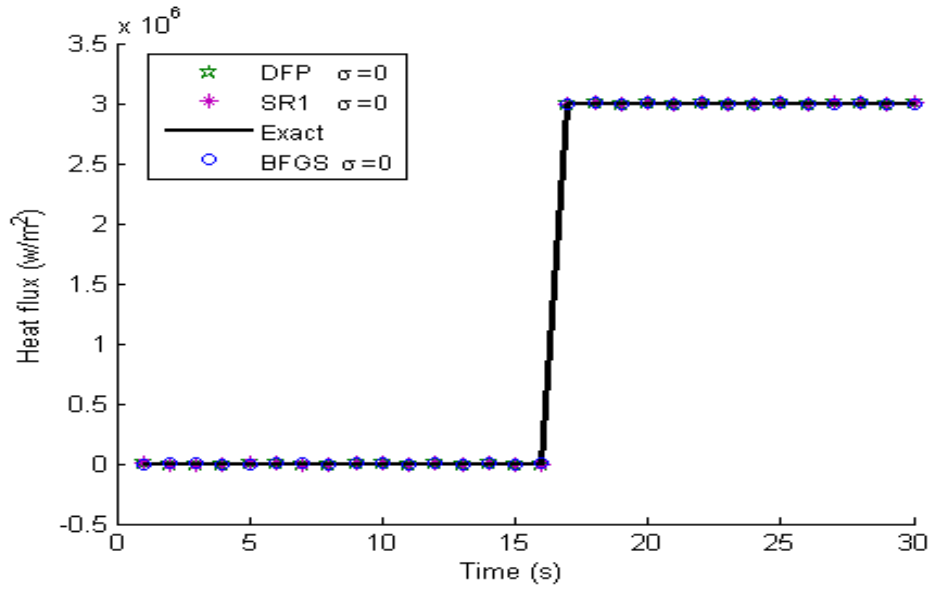


Figure 8. The estimation of the step heat flux with $\sigma = 0$

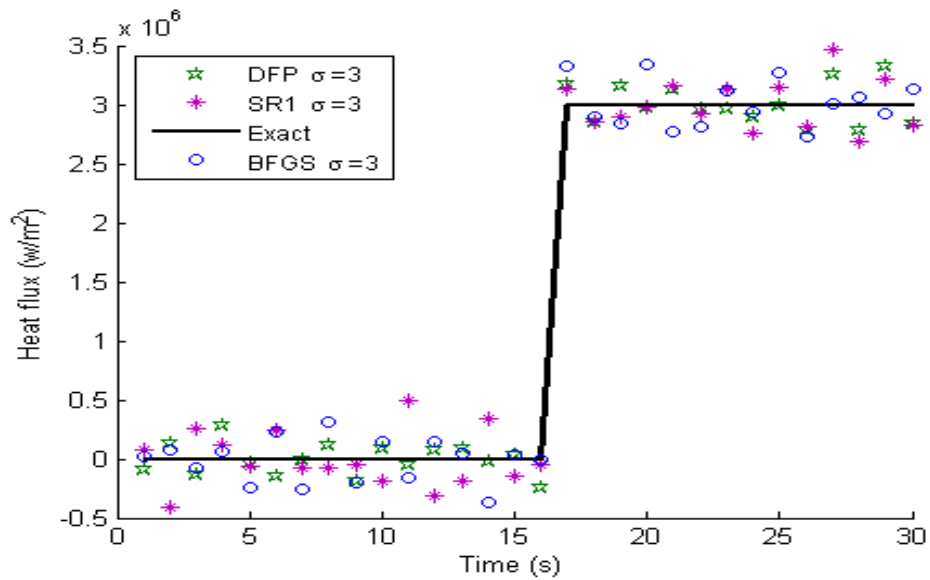


Figure 9. The estimation of the step heat flux with $\sigma = 3$

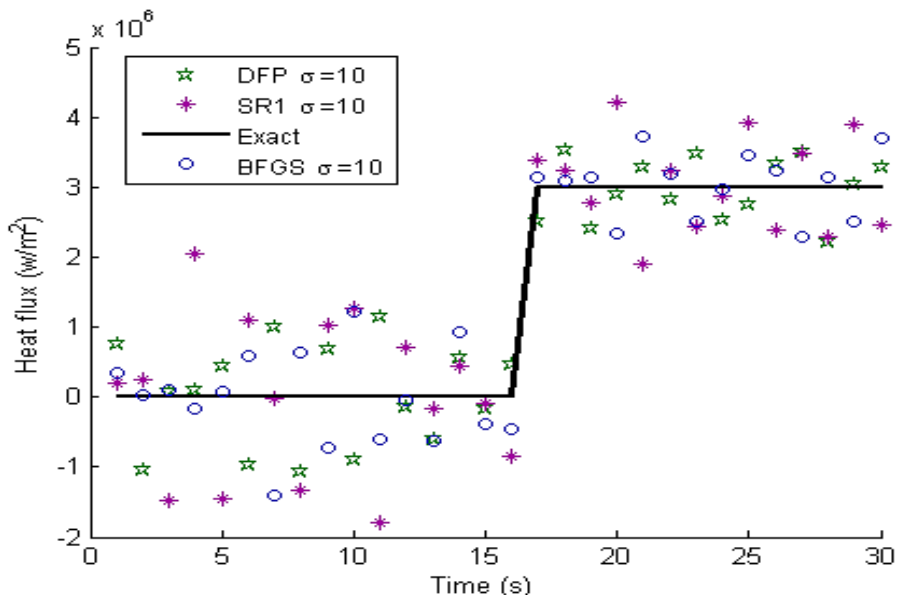


Figure 10. The estimation of the step heat flux with $\sigma = 10$

In this numerical test-case results are same to triangular heat flux and show that if the function of unknown heat flux is change suddenly, the DFP is better method for estimation of unknown heat flux than other two kinds. For utilize these inverse methods for design and analyze of nozzle we must show that the estimated flux by BFGS or DFP lead to same temperature distribution to real flux.

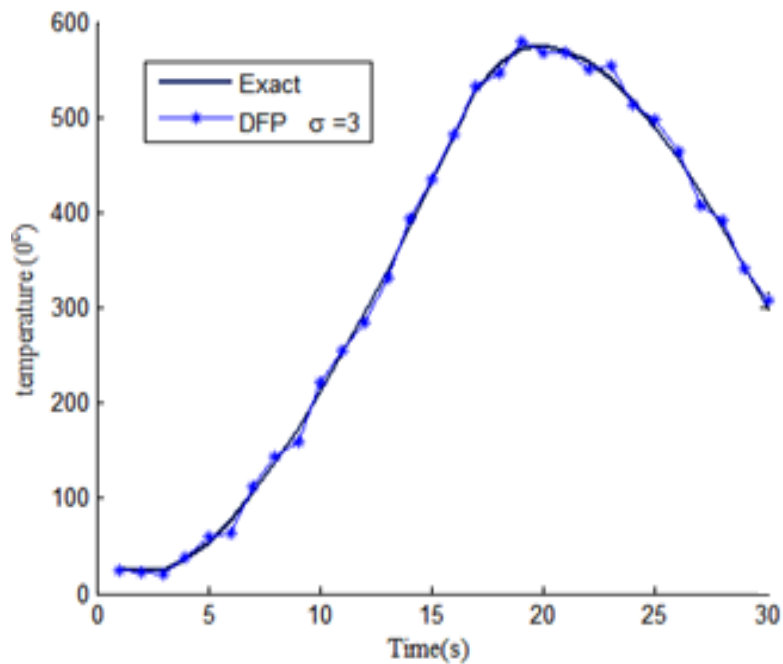


Figure 11. The exact and estimate temperature history at $x=1$ with $\sigma = 3$ (the triangular heat flux).

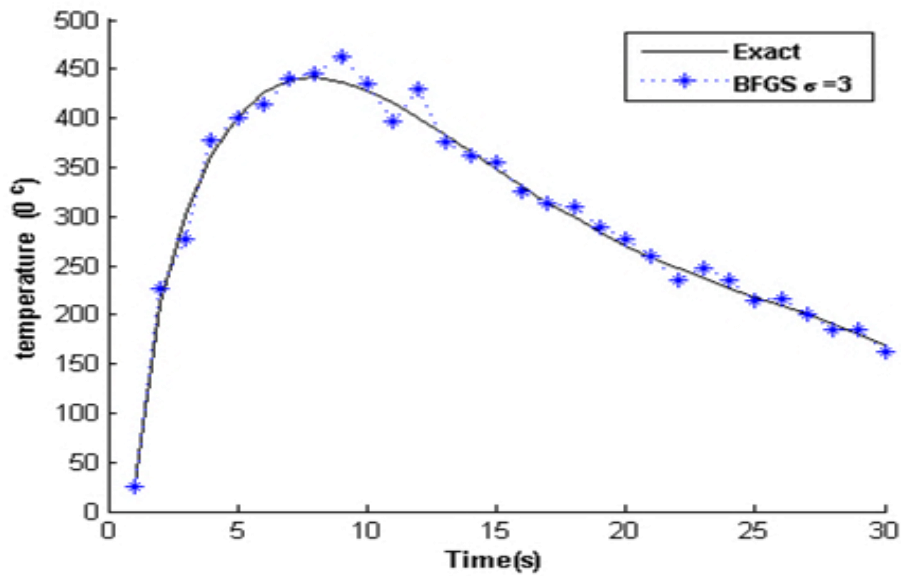


Figure 12. The exact and estimate temperature history at $x=1$ with $\sigma = 3$ (the third degree polynomial heat flux).

Figure 11 and 12 show that, the estimate temperature history (the temperature that calculate with estimate heat flux) at $x = 1$, have a good accuracy and could be used in engineering design for rocket nozzle.

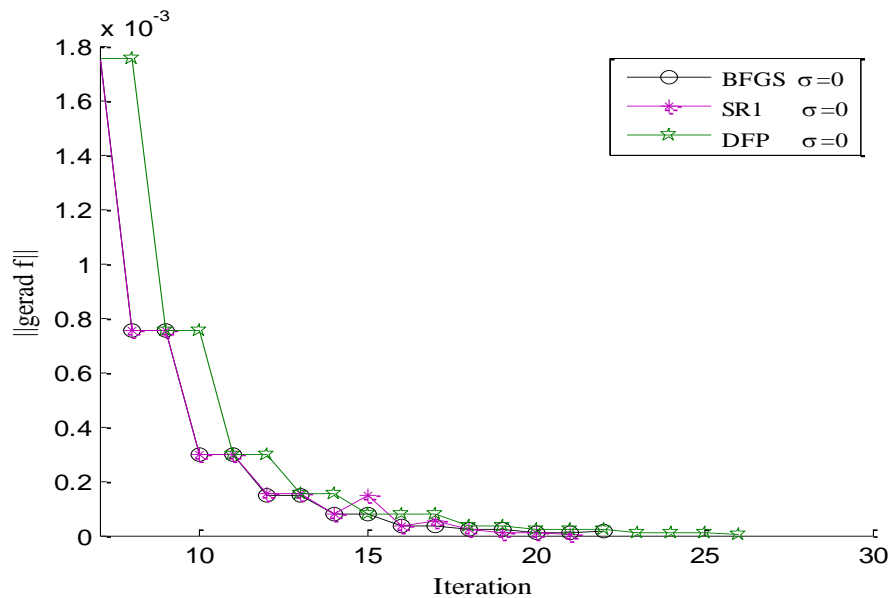


Figure 13. Trend for reduction of $\|\vec{\nabla}f\|$ after each iteration of VMM cycle with $\sigma = 0$ (the third degree polynomial heat flux).

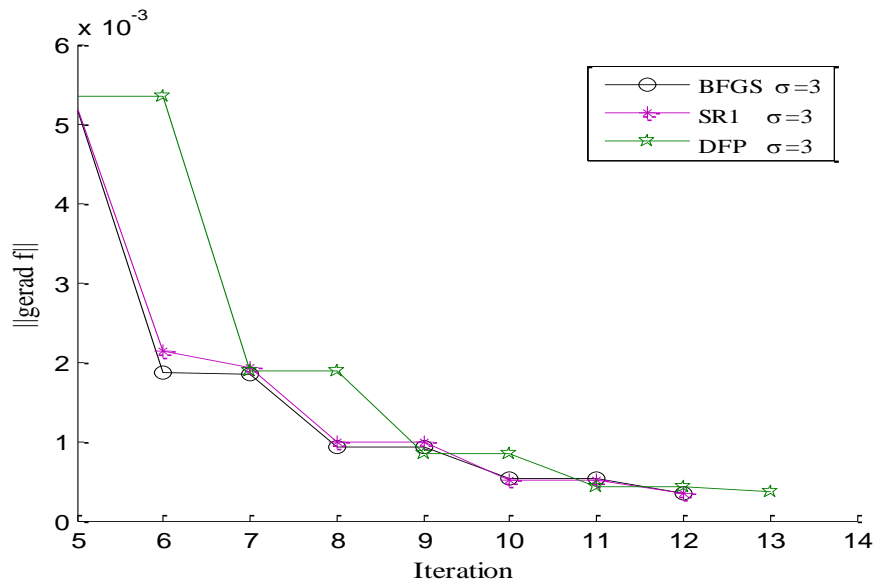


Figure 14. Trend for reduction of $\|\overline{\nabla}f\|$ after each iteration of VMM cycle with $\sigma = 3$ (the third degree polynomial heat flux).

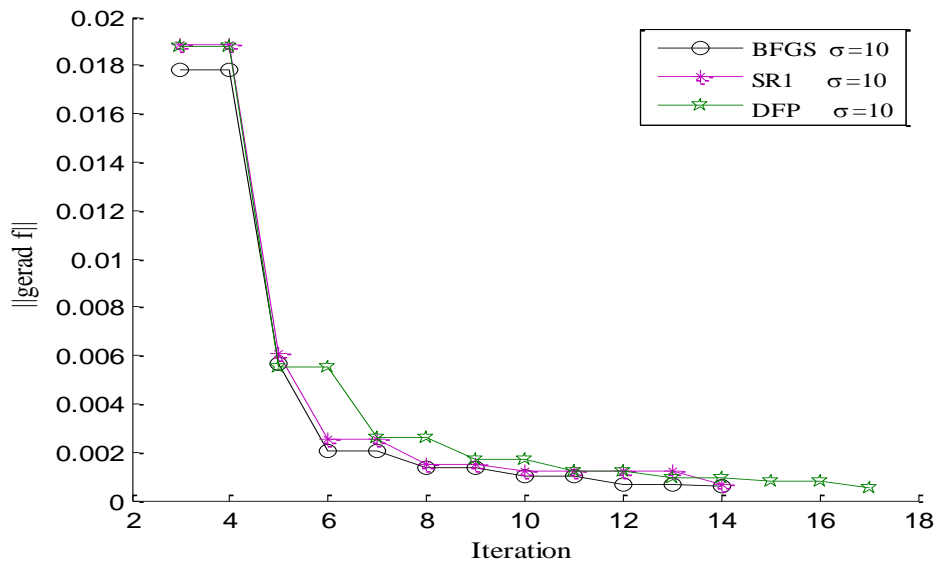


Figure 15. Trend for reduction of $\|\overline{\nabla}f\|$ after each iteration of VMM cycle with $\sigma = 0$ (the third degree polynomial heat flux).

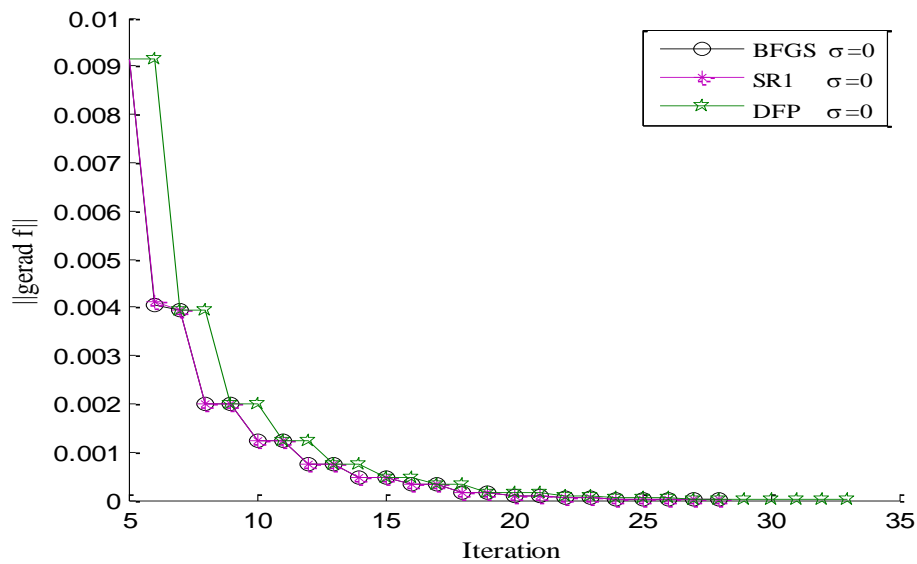


Figure 16. Trend for reduction of $\|\vec{\nabla}f\|$ after each iteration of VMM cycle with $\sigma = 0$ (the step heat flux).

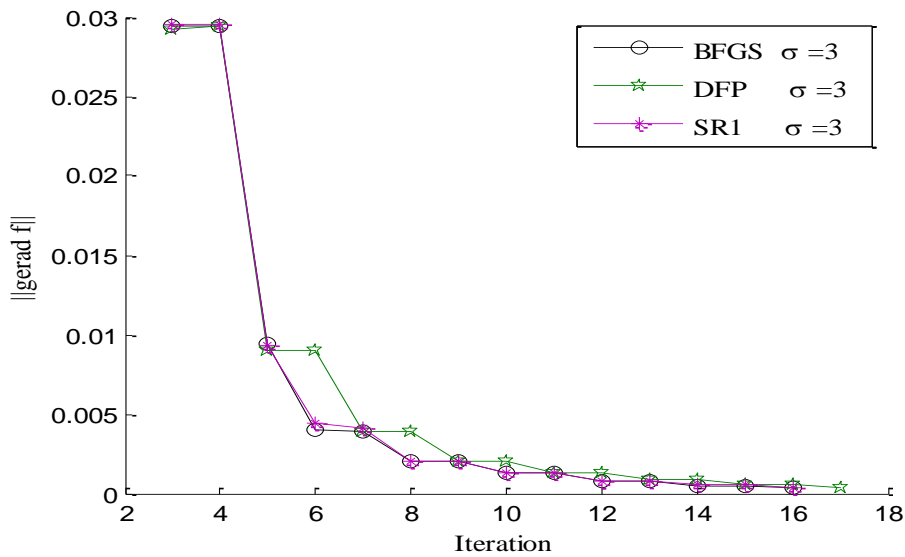


Figure 17. Trend for reduction of $\|\vec{\nabla}f\|$ after each iteration of VMM cycle with $\sigma = 3$ (the step heat flux)

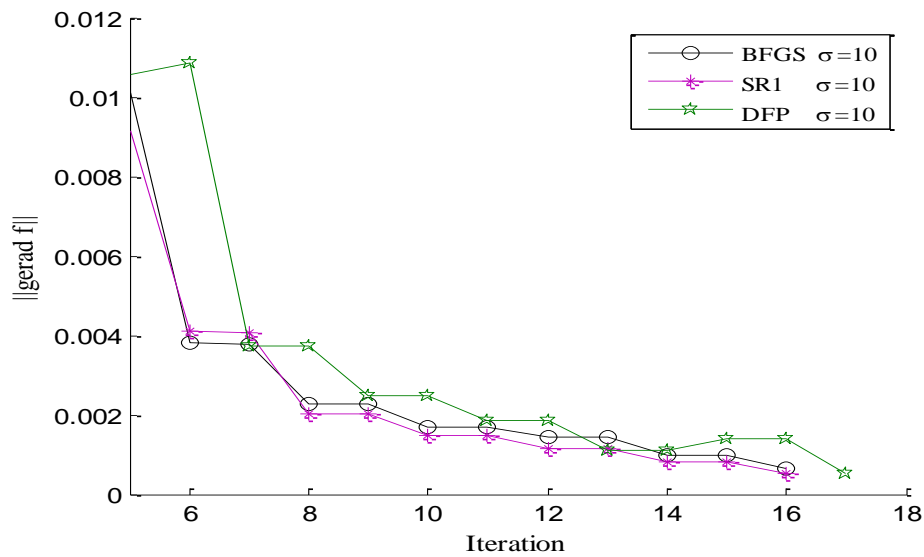


Figure 18. Trend for reduction of $\|\vec{\nabla}f\|$ after each iteration of VMM cycle with $\sigma = 10$ (the step heat flux)

Trend for reduction of $\|\vec{\nabla}f\|$ after each iteration can be seen in Figure 13 to Figure 18. This clearly shows BFGS converge with less iteration than DFP and almost SR1, the total time for estimate the third degree polynomial, the triangular and the step heat Flux by the BFGS is 83.6s and by SR1 is 84.63s and DFP is 88.54s, total times show that the SR1 rate for convergence is better than other version of the VMM. Total e_{rms} for estimate the third degree polynomial, the triangular and the step heat Flux with $\sigma = 0$, $\sigma = 3$, $\sigma = 10$ by the BFGS is 149.86 and the SR1 is 165.86 and finally by the DFP is 146.22.

6.0 CONCLUSIONS

Inverse heat conduction problem algorithms based on BFGS, SR1 and DFP were formulated in this paper. The various version of VMM was successfully applied for the solution of the inverse heat conduction problem in determining the unknown transient boundary heat flux by utilizing simulated temperature obtained from the boundary with measurement error. From the numerical test cases in this study it is concluded that the inverse solution obtained by using the technique of BFGS is best method for estimation of unknown function with uniform change, and for the function with sudden changes, the DFP has better convergence criteria than other two kinds.

7.0 REFERENCES

- Abboudi, S. and Artioukhine, A. (2002). Two dimensional computational estimation of transient boundary conditions for a flat specimen. In: *Proceedings of the fourth International Conference on Inverse Problems Engineering: Theory and Practice*, June 13–18, Rio, Brasil, ASME 2003.
- Bae, J.H. Hyun, J.M. and Kwak, H.S. (2004) Mixed convection from a multiblock heater in a channel with imposed thermal modulation, *Numerical Heat Transfer Part A*, 45, 329–345.
- Bauzin, J.G. and Laraqi, N. (2004) Simultaneous estimation of frictional heat flux and two thermal contact parameters for sliding contacts, *Numerical Heat Transfer* 45 (4) 313–328.
- Beck, J. V. Blackwell B. and St. Clair, C.R. (1985). *Inverse Heat Conduction-Ill Posed Problem*, Wiley: New York.
- Ch. H. H. and Wu, H. H. (2006). An Inverse Hyperbolic Heat Conduction Problem in Estimating Surface Heat Flux by the Conjugate Gradient Method, *Journal of Physics D: Applied Physics*, 39, 4087-4096.
- Daun KJ, Morton DP, Howell JR. (2003). Geometric optimization of radiant enclosures containing specular surfaces. *ASME Journal of Heat Transfer*, 125, 845 - 851.
- Franc-a FR., Howell J., Ezekoye OA., Morales JC. (2002). Inverse design of thermal systems. In: Hartnett JP, Irvine TF,(Ed.). *Advances in Heat Transfer*, (vol. 36. pp.1-110), New York: Elsevier.
- Hong, Y. K. and Baek, S.W. (2006). Inverse analysis for estimating the unsteady inlet temperature distribution for two-phase laminar flow in a channel, *Int. J. Heat Mass Transfer* , 49, 1137–1147.
- Huang C H and Chen (2000) A three-dimensional inverse forced convection problem in estimating surface heat flux by conjugate gradient method *Int. J. Heat Mass Transfer* 43 3171–81.
- Junxiang Shi, Jianhua Wang, (2009) Inverse problem of transpiration cooling for estimating wall heat flux by LTNE model and CGM method, *International Journal of Heat and Mass Transfer*, 52, 2714–2720
- Khoshkam, H. and Alizadeh M., (2011) Inverse problem of rocket nozzle throat for estimating inner wall heat flux by Broydon–Fletcher–Goldfarb–Shanno & conjugate gradient method, *International Review of Mechanical Engineering (I.R.E.M.E)*, 5(5)
- Kowsary, F. Behbahaninia, A. Pourshaghaghay, A. (2006). Transient heat flux function estimation utilizing the variable metric method, *International Communications in Heat and Mass Transfer*, 33, 800–810.

- Linhua L., Heping T. and Qizheng Y. (1999). Inverse radiation problem of temperature filed in three dimensional rectangular furnaces. *International Communications in Heat and Mass Transfer*; 26, 239 – 48.
- Lukšan L. and Spedicato E. (2000). Variable metric methods for unconstrained optimization and nonlinear least squares. *Journal of Computational and Applied Mathematics*, 124, 61 – 95.
- Patankar. S.V. (1980). *Numerical Heat Transfer and Fluid Flow*. New York: McGraw Hill
- Pourshaghagh, A. Kowsary, F. and Behbahaninia, A. (2007) Comparison of four different versions of the variable metric method for solving inverse heat conduction problems. *Heat Mass Transfer* 43, 285 – 294
- Prud'homme, M. and Jasmin, S. (2003). Determination of a heat source in porous medium with convective mass diffusion by an inverse method. *International Journal of Heat and Mass Transfer* 46 2065–2075.
- Rao S.S. (1995). *Optimization; Theory and Applications*. New Delhi: New Age International (P) Limited Publishers.
- Sparrow, E. M., Haji-Sheikh, A. and Lundgren, T.S. (1964). The Inverse Problem in Transient Heat Conduction, *ASME Journal of Applied Mechanics*, 86, 369-375.
- Stolz, G. Jr., (1960) Numerical Solutions to an Inverse Problem of Heat Conduction for Simpl Shapes, *ASME Journal of Heat Transfer*, 82, 20-26.
- Tikhonov A.N. and Arsenin, V.Y. (1977). *Solutions of Ill-Posed Problems*, Winston: Washington.
- Tsung-Chien Chen, Chiun-Chien Liu, (2008). Inverse estimation of heat flux and temperature on nozzle throat-insert inner contour, *International Journal of Heat and Mass Transfer*, 51, 3571–3581.
- Wang, H.N. and Wang, J.H. (2006). A numerical investigation of ablation and transpiration cooling using the local thermal non-equilibrium model [R], in: *Proceeding of the 42nd AIAA/ASME/SAE/ASEE Joint Propulsion Conference & Exhibit*, Sacramento, California, July 9–12, AIAA-5264.
- Wang, J.H., Wang, H.N., Sun, J.G. and Wang, J. (2007). Numerical simulation of control ablation by transpiration cooling, *Heat Mass Transfer*, 43, 471–478.
- Zhang, Z.Z., Cao, D.H. and Zeng, J.P. (2004). Property of a class of variable metric methods. *Applied Mathematics Letters* 17 , 437–442.